

Multi-focus Image Fusion: A Benchmark

Xingchen Zhang

Abstract—Multi-focus image fusion (MFIF) has attracted considerable interests due to its numerous applications. While much progress has been made in recent years with efforts on developing various MFIF algorithms, some issues significantly hinder the fair and comprehensive performance comparison of MFIF methods, such as the lack of large-scale test set and the random choices of objective evaluation metrics in the literature. To solve these issues, this paper presents a multi-focus image fusion benchmark (MFIFB) which consists a test set of 105 image pairs, a code library of 30 MFIF algorithms, and 20 evaluation metrics. MFIFB is the first benchmark in the field of MFIF and provides the community a platform to compare MFIF algorithms fairly and comprehensively. Extensive experiments have been conducted using the proposed MFIFB to understand the performance of these algorithms. By analyzing the experimental results, effective MFIF algorithms are identified. More importantly, some observations on the status of the MFIF field are given, which can help to understand this field better.

Index Terms—multi-focus image fusion, image fusion, benchmark, image processing, deep learning

I. INTRODUCTION

Clear images are desirable in computer vision applications. However, it is difficult to have all objects in focus in an image since most imaging systems have a limited depth-of-field (DOF). To be more specific, scene contents within the DOF remain clear while objects outside that area appear as blurred. Multi-focus image fusion (MFIF) aims to combine multiple images with different focused areas into a single image with everywhere in focus, as shown in Fig. 1.

MFIF has attracted considerable interests recently and various MFIF algorithms have been proposed, which can be generally divided into spatial domain-based methods and transform domain-based methods. Spatial domain-based methods operate directly in spatial domain and can be roughly divided into three categories: pixel-based [1], block-based [2] and region-based [3]. In contrast, transform domain-based methods firstly transform images into another domain and then perform fusion in that transformed domain. The fused image is then obtained via the inverse transformation. The representative transform domain-based methods are sparse representation (SR) methods [4, 5] and multi-scale methods [6, 7].

In recent years, with the development of deep learning, researchers have begun to solve the MFIF problem with deep learning techniques. Both supervised [9–12] and unsupervised MFIF algorithms [13–16] have been proposed. To be more specific, various deep learning models and methods have been employed, such as CNN [17, 18], GAN [19] and ensemble learning [20].

X. Zhang is with the Department of Electrical and Electronic Engineering, Imperial College London, London, United Kingdom. e-mail: xingchen.zhang@imperial.ac.uk

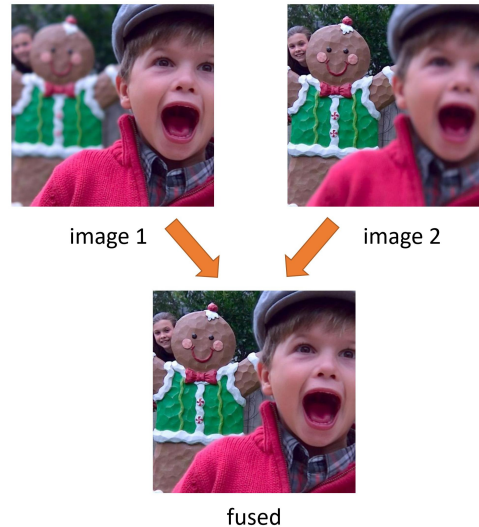


Fig. 1. The benefit of multi-focus image fusion. In image 1, the background is not clear while in image 2 the foreground is not clear. After fusion, both the background and foreground in the fused image are clear. The fused image is produced by CBF [8].

However, current research on MFIF is suffering from several issues, which hinder the development of this field severely. First, there is not a well-recognized MFIF benchmark which can be used to compare performance under the same standard. Therefore, it is quite common that different images are utilized in experiments in the literature, which makes it difficult to fairly compare the performance of various algorithms. Although the Lytro dataset [33] is used frequently, many researchers only choose several image pairs from it in experiments, resulting in bias results. This is very different from other image processing-related areas like visual object tracking where several benchmarks [34, 35] are available and every paper has to show results on some of them. Second, as the most widely used dataset, the Lytro dataset only consists of 20 pairs of multi-focus images which are not enough for large-scale comparison. Also, Xu et al. [36] showed that the defocus spread effect (DSE) is not obvious in Lytro dataset thus popular methods perform very similar on it. Third, although many evaluation metrics have been proposed to evaluate the image fusion algorithms, none of them is better than all other metrics. As a result, researchers normally choose several metrics which support their methods in the literature. This makes it not trivial to compare performances objectively. Table I lists some algorithms published in top journals (conferences) and the number of image pairs, compared algorithms, and evaluation metrics. As can be seen, these works present results of different evaluation metrics on different number of image pairs, making it quite difficult to ensure a fair and comprehen-

TABLE I

SOME MFIF ALGORITHMS PUBLISHED IN TOP JOURNALS AND CONFERENCES. THE NUMBER OF TESTED IMAGE PAIRS, THE NUMBER OF COMPARED ALGORITHMS, THE NUMBER OF UTILIZED EVALUATION METRICS ARE ALSO GIVEN. THE DETAILS OF THE PROPOSED MFIFB ARE ALSO SHOWN.

Reference	Year	Journal	Image pairs	Algorithms	Metrics
GFF [21]	2013	IEEE Transactions on Image Processing	10	7	5 (MI, Q_Y , Q_C , Q_G , Q_P)
RP_SR [22]	2015	Information Fusion	10	8	5 (SD, EN, Q_G , Q_P , Q_W)
MST_SR [22]	2015	Information Fusion	10	8	5 (SD, EN, Q_G , Q_P , Q_W)
NSCT_SR [22]	2015	Information Fusion	10	8	5 (SD, EN, Q_G , Q_P , Q_W)
QB [23]	2015	Information Fusion	6	N/A	3 (Q_{GM} , $Q^{AB/F}$, NMI)
DSIFT [1]	2015	Information Fusion	12	9	6 (NMI, Q_{NCIE} , Q_G , PC, Q_Y , Q_{CB})
MRSR [24]	2016	IEEE Transactions on Image Processing	7	9	4 (MI, Q_G , ZNCC_PC, Q_{PC})
CNN [25]	2017	Information Fusion	40	6	4 (NMI, $Q^{AB/F}$, Q_Y , Q_{CB})
BFMF [26]	2017	Information Fusion	18	6	4 (NMI, PC, Q_{MSSI} , Q_C)
[5]	2018	Information Fusion	10	9	5 (MI, Q_G , Q_S , Q_{ZP} , Q_{PC})
p-CNN [27]	2018	Information Science	12	5	4 (NMI, Q_{PC} , Q_W , Q_{CB})
CAB [28]	2019	Information Fusion	34	15	5 ($Q^{AB/F}$, NMI, FMI, Q_Y , Q_{NCIE})
mf-CRF [29]	2019	IEEE Transactions on Image Processing	52	11	4 (MI, Q_G , Q_Y , Q_{CB})
DIF-Net [16]	2020	IEEE Transactions on Image Processing	20	9	7 (MI, FMI, Q_X , Q_{SCD} , Q_H , Q_P , Q_M)
DRPL [30]	2020	IEEE Transactions on Image Processing	20	7	5 (MI, $Q^{AB/F}$, AG, VIF, EI)
IFCNN [10]	2020	Information Fusion	20	4	5 (VIF, ISSIM, NMI, SF, AG)
FusionDN [31]	2020	AAAI	10	5	4 (SD, EN, VIF, SCD)
PMGI [32]	2020	AAAI	18	5	6 (SSIM, $Q^{AB/F}$, EN, FMI, SCD, CC)
MFIFB	2020		105	30	20 (CE, EN, FMI, NMI, PSNR, Q_{NCIE} , TE, AG, EI, $Q^{AB/F}$, Q_P , SD, SF, Q_C , Q_W , Q_Y , SSIM, Q_{CB} , Q_{CV} , VIF)

side performance comparison. Besides, many researchers only choose several algorithms which may be outdated to compare with their own algorithms, making it more difficult to know the real performance of these algorithms. More importantly, it is frequent that methods are compared with those which are not designed for this task [37]. For example, the performance of a MFIF algorithm is compared with a method designed for visible-infrared image fusion. Finally, although the source codes of some MFIF algorithms have been made publicly available, the usage of these codes are different. For examples, different codes have different interfaces to read and write images, and may have various dependencies to install. Therefore, it is inconvenient and time-consuming to conduct large scale performance evaluation. It is thus desirable that results on public datasets are available and a consistent interface is available to integrate new algorithms conveniently for performance comparison.

To solve these issues, in this paper a multi-focus image fusion benchmark (MFIFB) is created, which includes 105 pairs of multi-focus images, 30 publicly available fusion algorithms, 20 evaluation metrics and an interface to facilitate the algorithm running and performance evaluation. The main contributions of this paper lie in the following aspects:

- **Dataset.** A test set containing 105 pairs of multi-focus images is created. These image pairs cover a wide range of environments and conditions. Therefore, the test set is able to test the generalization ability of fusion algorithms.
- **Code library.** 30 recent MFIF algorithms are collected and integrated into a code library, which can be easily utilized to run algorithms and compare performances. An

interface is designed to integrate new image fusion algorithms into MFIFB. It is also convenient to compare performances using fused images produced by other algorithms with those available in MFIFB.

- **Comprehensive performance evaluation.** 20 evaluation metrics are implemented in MFIFB to comprehensively compare fusion performance. This is much more than those utilized in the MFIF literature as shown in Table I. Extensive experiments have been conducted using MFIFB, and the comprehensive comparison of those algorithms are performed.

The rest of this paper is organized as follows. Section II gives some background information about MFIF. Then, the proposed multi-focus image fusion benchmark is introduced in detail in Section III, followed by experiments and analysis in Section IV. Finally, Section V concludes the paper.

II. MULTI-FOCUS IMAGE FUSION METHODS

A. The background of multi-focus image fusion

MFIF aims to produce an all-in-focus image by fusing multiple partially focused images of the same scene [38]. Normally, MFIF is solved by combining focused regions with some fusion rules. The key task in MFIF is thus the identification of focused and defocused area, which is normally formulated as a classification problem.

Various focus measurements (FM) were designed to classify whether a pixel is focused or defocused. For example, Zhai et al. [9] used the energy of Laplacian to detect the focus level of source images. Tang et al. [27] proposed a pixel-wise

convolutional neural network (p-CNN) which was a learned FM that can recognize the focused and defocused pixels.

B. Conventional multi-focus image fusion methods

Generally speaking, conventional MFIF algorithms can be divided into spatial domain-based methods and transform domain-based methods. Spatial domain-based methods operate directly in spatial domain. According to the adopted ways, these methods can be classified as pixel-based [1], block-based [2] and region-based [3]. In pixel-based methods, the FM is applied at pixel-level to judge whether a pixel is focused or defocused. In block-based methods, the source images are firstly divided to blocks with fixed size, and then the FM is applied to these patches to decide their blurring levels. However, the performance of block-based methods heavily dependent on the division of blocks and may induce artifacts easily. In region-based methods, the source images are firstly segmented into different regions using segmentation techniques, and then the blurring levels of these regions are calculated based on FM.

The transform domain-based methods normally consist of three steps. First, the source images are transformed to another domain using some transformations, such as wavelet transform and sparse representation. The source images can be represented using some coefficients in this way. Second, the coefficients of source images are fused using designed fusion rules. Finally, the fused image is obtained by applying inverse transformation to those fused coefficients. Transform domain-based algorithms mainly contain sparse representation-based [39, 40], multi-scale-based [41, 42], subspace-based [43], edge-preserving-based [44, 45] and others.

C. Deep learning-based methods

In recent years, deep learning has been applied to MFIF and an increasing number of deep learning-based methods emerge every year. Liu et al. [25] proposed the first CNN-based method which utilized a CNN to learn a mapping from source images to the focus map. Since then, more than 40 deep learning-based MFIF algorithms have been proposed.

The majority of deep learning-based MFIF algorithms are supervised algorithms, which need a large amount of training data with ground-truth to train. For instance, Zhao et al. [46] developed a MFIF algorithm based on multi-level deeply supervised CNN (MLCNN). Tang et al. [27] proposed a pixel-wise convolutional neural network (p-CNN) which was a learned FM that can recognize the focused and defocused pixels in source images. Yang et al. [47] proposed a multi-level features convolutional neural network (MLFCNN) architecture for MFIF. Li et al. [30] proposed the DRPL, which directly converts the whole image into a binary mask without any patch operation. Zhang et al. [10] proposed a general image fusion framework based on CNN (IFCNN).

In supervised learning-based methods, a large amount of labeled training data is needed, which is labor-intensive and time-consuming. To solve this issue, researchers have began to develop unsupervised MFIF algorithms. For example, Yan et al. [13] proposed the first unsupervised MFIF algorithm based

on CNN, namely MFNet. The key to achieve unsupervised training in that work was the usage of a loss function based on SSIM, which is a widely used image fusion evaluation metric that measures the structural similarity between source images and the fused image. Ma et al. [14] proposed an unsupervised MFIF algorithm based on an encoder-decoder network (SESF), which also utilized SSIM as a part of the loss function. Other unsupervised methods include DIF-Net [16] and FusionDN [31].

Apart from CNN, some other deep learning models have also been utilized to perform MFIF. For example, Guo et al. [19] presents the first GAN-based MFIF algorithm (FuseGAN). Deshmukh et al. [48] proposed to use deep belief network (DBN) to calculate weights indicating the sharp regions of input images. Unlike above-mentioned methods which only use one model in their methods, Naji et al. [20] proposed a MFIF algorithm based on the ensemble of three CNNs.

III. MULTI-FOCUS IMAGE FUSION BENCHMARK

As presented previously, in most MFIF works, the algorithm were tested on a small number of images and compared with a very limited number of algorithms using just several evaluation metrics. This makes it difficult to comprehensively evaluate the real performance of these algorithms. This section presents a multi-focus image fusion benchmark (MFIFB), including the dataset, baseline algorithms, and evaluation metrics.

A. Dataset

The dataset in MFIFB is a test set including 105 pairs of multi-focus images. Each pair consists of two images with different focus areas. Because most researches in MFIF are about fusing two images, therefore at the moment only image pairs consisting of two images are collected in MFIFB. Since this paper aims to create a benchmark in the field of MFIF, thus to maximize its value, this test set consists of existing datasets which do not have code library and results. Specifically, the test set is collected from Lytro [33], MFFW [36], the dataset of Savic et al. [49], Aymaz et al. [50], and Tsai et al.¹. By doing this, we not only provide benchmark results on the whole dataset, but also give benchmark results for these existing datasets, which will make it more convenient for researchers who are familiar with these datasets to compare results.

The images included in MFIFB are captured with various cameras at various places, and they cover a wide range of environments and working conditions. The resolutions of images vary from 178×134 to 1024×768 . Therefore, these images can be used to test the performance of MFIF algorithms comprehensively. Table II lists more details about different kinds of images included in MFIFB.

TABLE II
THE NUMBER OF DIFFERENT KINDS OF IMAGES IN MFIFB.

Category	Color/gray	Real/simulated	Registered/not well registered
Number	71/34	64/41	98/7

¹<https://www.mathworks.com/matlabcentral/fileexchange/45992-standard-images-for-multifocus-image-fusion>

TABLE III
MULTI-FOCUS IMAGE FUSION ALGORITHMS THAT HAVE BEEN INTEGRATED IN MFIFB.

Category	Method	
Spatial domain-based	BFMF [26], BGSC [51], DSIFT [1], IFM [56], QB [23], TF [64]	
Transform domain-based	SR-based	ASR [40], CSR [52]
	Multi-scale-based	CBF [8], DCT_Corr [6], DCT_EOL [6], DWTDE [53], GD [54], MSVD [59], MWGF [60], SVDDCT [63]
	edge-preserving-based	GFDF [55], GFF [21], MFM [57], MGFF [58]
	subspace-based	SFMD [62]
Hybrid	MST_SR [22], NSCT_SR [22], RP_SR [22]	
Deep learning-based	Supervised	CNN [25], DRPL [30], ECNN [20], IFCNN [10], PCANet [61]
	Unsupervised	SESF [14]

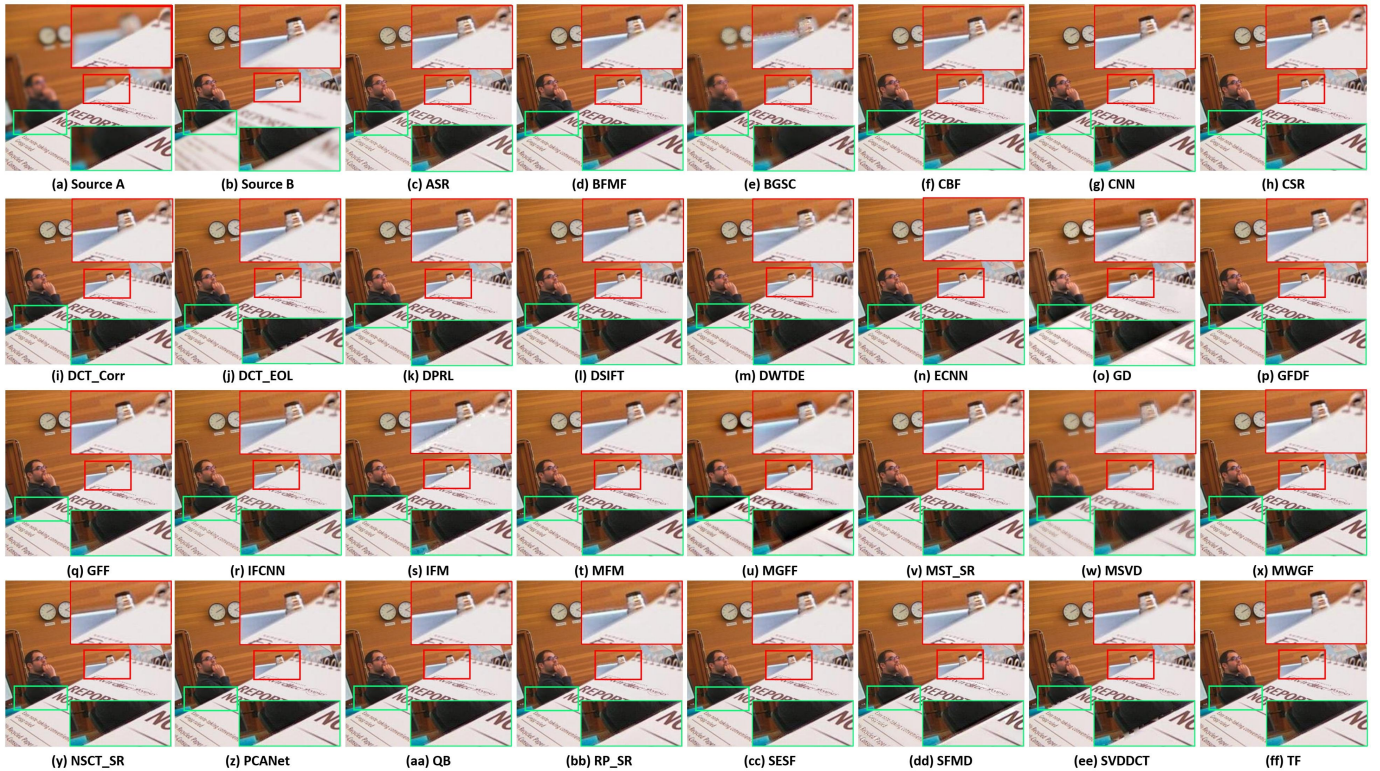


Fig. 3. The source images and fused images of *Lytro19* image pair. (a) and (b) are the source images. From (c) to (ff) are the fused images produced by 30 integrated MFIF algorithms in MFIFB. The magnified plot of area within red box near the focused/defocused boundary are given at the top right corner of each fused image. The magnified plot of area within green box near the focused/defocused boundary are given at the bottom right corner of each fused image.

to produce results and compare performances. To integrate algorithms into MFIFB and for the convenience of users, an interface was designed to integrate more algorithms into MFIFB. Besides, for researchers who do not want to make their codes publicly available, they can simply put their fused images into MFIFB and then their algorithms can be compared with those integrated in MFIFB easily.

C. Evaluation metrics

The assessment of MFIF algorithms is not a trivial task since the ground-truth images are normally not available. Generally there are two ways to evaluate MFIF algorithms, namely subjective or qualitative method and objective or quantitative method.

Subjective evaluation means that the fusion performance is evaluated by human observers. This is very useful in MFIF research since a good fused image should be friendly to human visual system. However, it is time-consuming and labor-intensive to observe each fused image in practice. Besides, because each observer has different standard when observing fused images, thus biased evaluation may be easily produced. Therefore, qualitative evaluation alone is not enough for the fusion performance evaluation. Therefore, objective evaluation metrics are needed for quantitative comparison.

As introduced in [65], image fusion evaluation metrics can be classified into four types as

- Information theory-based

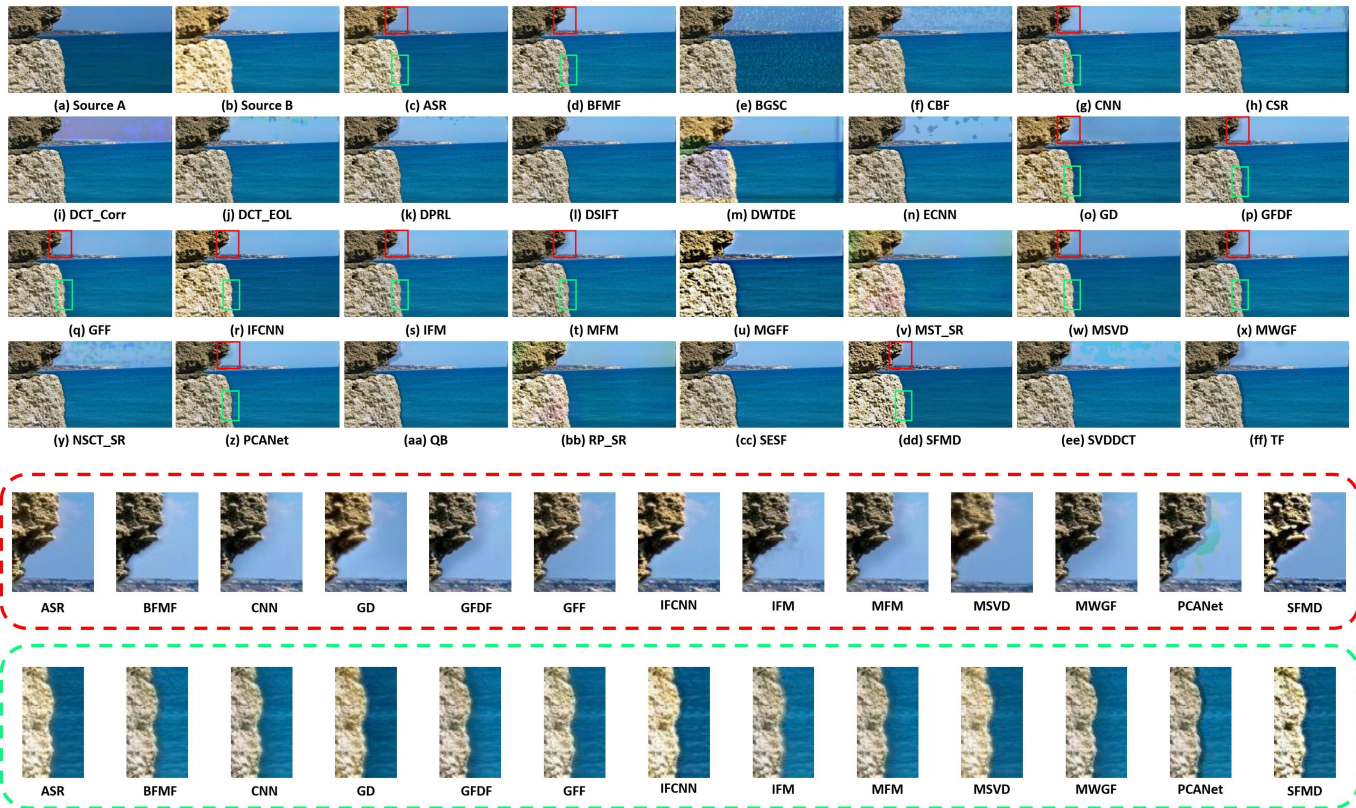


Fig. 4. The source images and fused images of *MMFW12* image pair. (a) and (b) are the source images. From (c) to (ff) are the fused images produced by 30 integrated MFIF algorithms in MFIFB. The magnified plot of area within red box near the focused/defocused boundary are given in the red dash box. The magnified plot of area within green box near the focused/defocused boundary are given in the green dash box.

- Image feature-based
- Image structural similarity-based
- Human perception inspired

Numerous evaluation metrics for image fusion have been proposed. However, none of them is better than all other metrics. To have comprehensive and objective performance comparison, 20 evaluation metrics were implemented in MFIFB². The evaluation metrics integrated in MFIFB cover all four categories of metrics, thus are capable of quantitatively showing the quality of a fused image. Specifically, the implemented information theory-based metrics include cross entropy (CE) [66], entropy (EN) [67], feature mutual information (FMI), normalized mutual information (NMI) [68], peak signal-to-noise ratio (PSNR) [69], nonlinear correlation information entropy (Q_{NCIE}) [70, 71], and tsallis entropy (TE) [72]. The implemented image feature-based metrics include average gradient (AG) [73], edge intensity (EI) [74], gradient-based similarity measurement ($Q^{AB/F}$) [75], phase congruency (Q_P) [76], standard deviation (SD) [77] and spatial frequency (SF) [78]. The implemented image structural similarity-based metrics include Cvejie’s metric Q_C [79], Peilla’s metric (Q_W) [80], Yang’s metric (Q_Y) [81], and structural similarity index measure (SSIM) [82]. The implemented human perception

inspired fusion metrics are human visual perception (Q_{CB}) [83], Q_{CV} [84] and VIF [85].

Due to the page limitation, the mathematical expression of these metrics are not given here. For all metrics except CE and Q_{CV} , a larger value indicates a better fusion performance. In MFIFB, it is convenient to compute all these metrics for each method, making it easy to compare performances. Note that many metrics are designed for gray images. In this work, each metric was computed for every channel of RGB images and then the average value was computed. More information about evaluation metrics can be founded in [65, 69, 86].

IV. EXPERIMENTS AND ANALYSIS

This section presents experimental results within MFIFB. All experiments were performed using a computer equipped with an NVIDIA RTX2070 GPU and i7-9750H CPU. Default parameters reported by the corresponding authors of each algorithm were employed. Note that pre-trained models of each deep learning algorithm were provided by the corresponding authors of each algorithm. The dataset in MFIFB is only used for performance evaluation of those algorithms but not for the training.

A. Results on the Lytro dataset

Many papers utilize Lytro in the experiments, thus the Lytro dataset is collected as a subset in MFIFB and in this Section

²The implementation of some metrics are kindly provided by Zheng Liu at <https://github.com/zhengliu6699/imageFusionMetrics>

TABLE IV
AVERAGE EVALUATION METRIC VALUES OF ALL METHODS ON THE LYTRO DATASET (20 IMAGE PAIRS). THE BEST THREE VALUES IN EACH METRIC ARE DENOTED IN RED, GREEN AND BLUE, RESPECTIVELY. THE THREE NUMBERS AFTER THE NAME OF EACH METHOD DENOTE THE NUMBER OF BEST VALUE, SECOND BEST VALUE AND THIRD BEST VALUE, RESPECTIVELY. BEST VIEWED IN COLOR.

Method	CE	EN	FMI	NMI	PSNR	Q _{NRCTE}	TE	AG	EI	Q _{A/B/F}	Q _P	SD	SF	Q _C	Q _{IV}	Q _X	SSIM	Q _{CB}	Q _{CV}	VIF
BMPF (0.1,0)	0.019638	7.52490	0.89989	1.08842	64.61350	0.83450	77.42350	6.84384	71.10150	0.73952	0.81329	61.32400	19.18350	0.80916	0.92867	0.92718	1.66988	0.79153	22.220	0.93554
BGSC (1.0,0)	0.015494	7.50940	0.882147	0.92492	64.81300	0.831577	46.64590	5.49728	55.58600	0.517730	0.46380	59.44600	15.94270	0.75469	0.73499	0.74703	1.64030	0.65819	11.37760	0.72425
DSFT (0.2,2)	0.020353	7.54410	0.89770	1.09688	64.41200	0.835710	78.01500	6.81163	72.04680	0.48613	0.818027	61.88300	19.48700	0.811880	0.948615	0.947128	1.66796	0.780715	16.75150	0.93778
FM (0.0,0)	0.020499	7.52830	0.89794	1.06879	64.45880	0.839274	73.18050	6.91470	71.97200	0.730629	0.791069	61.31200	19.45460	0.80384	0.937143	0.949629	1.66620	0.782972	21.31200	0.93032
FM (1.0,5)	0.020324	7.52025	0.89988	1.09809	64.44380	0.839274	78.160430	6.92465	71.97200	0.730629	0.815647	61.80000	19.46360	0.811833	0.945104	0.974253	1.66835	0.796637	17.69450	0.93697
TF (2.5,5)	0.020177	7.52095	0.89991	1.09800	64.57280	0.838992	77.01250	6.90815	71.25150	0.74418	0.819235	61.55250	19.46910	0.812919	0.947748	0.974406	1.67050	0.795914	16.82020	0.937495
ASR (0.2,2)	0.019154	7.52745	0.898110	0.90682	64.92970	0.839590	77.95950	6.77825	71.25150	0.724654	0.809586	60.92400	19.06720	0.80111	0.943607	0.949496	1.67196	0.710252	27.03780	0.89737
ASR (1.0,0)	0.020266	7.52795	0.899603	1.03608	64.57860	0.835017	62.05820	6.85940	71.08590	0.732571	0.794129	61.49010	19.52170	0.794129	0.946077	0.949537	1.67038	0.768753	16.56690	0.93281
CBF (0.2,0)	0.019302	7.52065	0.897206	0.976413	64.57310	0.839661	48.33450	6.72625	69.76070	0.732017	0.793537	60.90730	18.67610	0.808502	0.935265	0.935327	1.69230	0.749864	26.24500	0.934010
DCT (0.0,0)	0.020061	7.52730	0.899367	1.08972	64.54780	0.839064	67.49050	6.92705	71.90150	0.740526	0.809592	61.50160	19.42950	0.80230	0.93470	0.936833	1.667025	0.787151	21.48700	0.934540
DCT_B0L (0.0,0)	0.020249	7.52735	0.899547	1.09470	64.54160	0.839282	77.50910	6.93225	72.00000	0.742823	0.810574	61.55200	19.46070	0.810006	0.938988	0.956555	1.667215	0.789194	20.11730	0.933844
DWTDE (0.1,0)	0.019597	7.52795	0.898809	1.06658	64.60670	0.835793	67.52400	6.75260	70.10950	0.716554	0.784280	61.20400	18.92690	0.80234	0.932183	0.952613	1.667810	0.767808	29.08350	0.931895
GD (3.0,0)	0.026776	7.607335	0.887266	0.911936	61.272450	0.831166	67.52400	6.90210	71.74680	0.697429	0.693197	57.30650	18.02430	0.723460	0.869108	0.838173	1.557468	0.688432	127.11960	1.000538
MSPD (2.0,0)	0.026384	7.49740	0.879994	0.789597	65.24750	0.822690	44.96890	4.80190	49.52500	0.502233	0.518128	58.54500	14.43330	0.724487	0.748462	0.790878	1.692465	0.604281	86.14970	0.748725
MWGF (1.0,0)	0.020377	7.52725	0.895568	0.940344	64.54050	0.837937	71.92580	6.815705	70.87600	0.732472	0.809721	61.46920	19.25750	0.809685	0.929581	0.973900	1.668208	0.783379	19.69900	0.928066
SYDDCT (0.0,0)	0.020117	7.526470	0.896566	1.094793	64.54350	0.839381	78.37690	6.92790	71.95200	0.742519	0.811085	61.55500	19.46560	0.806462	0.941773	0.969724	1.667475	0.788470	18.02500	0.934666
GFDF (2.2,3)	0.020140	7.526160	0.899992	1.090750	64.57310	0.838961	77.34450	6.92755	71.70000	0.745001	0.818468	61.54930	19.39700	0.812099	0.947740	0.974458	1.670630	0.796594	16.64080	0.937175
GFDF (0.0,0)	0.020287	7.529880	0.899365	1.04995	64.61200	0.835995	64.04050	6.801830	71.55280	0.742155	0.815251	61.46380	19.47270	0.814630	0.946958	0.969402	1.670730	0.782379	17.19130	0.934930
MFM (1.0,1)	0.020050	7.526425	0.899556	1.08307	64.53670	0.838992	76.91070	6.89880	71.65400	0.745218	0.817426	61.57200	19.46810	0.813455	0.948587	0.974237	1.670915	0.794728	17.40530	0.935602
MGFF (1.1,1)	0.046011	7.534860	0.887996	0.766430	64.01650	0.821880	26.07950	6.187375	64.49450	0.644779	0.671019	63.21800	17.44950	0.773243	0.898198	0.872198	1.671740	0.652563	58.17590	0.975855
SFMD (3.2,1)	0.031383	7.535650	0.886008	0.759886	63.59470	0.821765	24.30030	8.153865	84.40340	0.640447	0.680628	62.95500	23.44900	0.772858	0.889099	0.896568	1.624320	0.656672	77.41900	0.949093
MST_SR (1.0,1)	0.022262	7.528345	0.890967	0.952416	64.60150	0.830625	43.77650	6.93220	71.99800	0.733014	0.806941	61.76530	19.44520	0.805785	0.947812	0.956312	1.669545	0.756733	19.61030	0.946196
NSCT_SR (0.0,0)	0.020021	7.52815	0.899531	1.059497	64.61200	0.837055	69.12880	6.90870	71.76300	0.741461	0.814431	61.43830	19.39950	0.810613	0.947641	0.966277	1.671110	0.781873	16.89540	0.934884
RP_SR (1.0,0)	0.022805	7.529890	0.895937	0.923847	64.60710	0.829275	68.96820	6.92845	71.89220	0.720292	0.776160	61.649750	19.53860	0.80218	0.946219	0.964780	1.671150	0.738752	20.64050	0.939251
CNN (0.0,3)	0.019920	7.526245	0.899765	1.082380	64.60280	0.838458	75.47250	6.875200	71.40820	0.744251	0.818436	61.49530	19.29890	0.812681	0.946088	0.973324	1.672075	0.794012	17.10870	0.935537
DPRL (0.1,2)	0.020867	7.528040	0.890982	1.017829	64.549050	0.834265	56.28700	6.959190	72.024350	0.737734	0.817047	61.59190	19.51940	0.810714	0.946652	0.971286	1.668705	0.797367	17.73470	0.937124
ECNN (3.2,0)	0.020178	7.529390	0.900061	1.01154	64.53670	0.839672	80.749550	6.911405	71.75880	0.741015	0.805103	61.80400	19.46200	0.810527	0.944447	0.970987	1.667370	0.792449	16.82140	0.933466
FCNN (0.0,0)	0.037096	7.530980	0.898192	0.968276	63.38820	0.829690	6.93380	6.93380	71.98930	0.712780	0.817183	61.44400	19.44240	0.803788	0.942935	0.938947	1.670895	0.790921	18.83240	0.934636
PCANet (0.0,1)	0.020317	7.524715	0.900045	1.087111	64.53190	0.838525	76.624150	6.800480	71.47150	0.738438	0.814058	61.55090	19.39540	0.810176	0.939627	0.973351	1.669560	0.792703	16.99950	0.934086
SESF (0.0,0)	0.020269	7.526615	0.899455	1.081988	64.541250	0.838440	77.49390	6.909350	71.78860	0.739873	0.811905	61.58810	19.45670	0.809254	0.946288	0.971380	1.668120	0.793740	18.02370	0.938644

TABLE V
AVERAGE EVALUATION METRIC VALUES OF ALL METHODS ON THE WHOLE MF10B DATASET (105 IMAGE PAIRS). THE BEST THREE VALUES IN EACH METRIC ARE DENOTED IN RED, GREEN AND BLUE, RESPECTIVELY. THE THREE NUMBERS AFTER THE NAME OF EACH METHOD DENOTE THE NUMBER OF BEST VALUE, SECOND BEST VALUE AND THIRD BEST VALUE, RESPECTIVELY. BEST VIEWED IN COLOR.

Method	CE	EN	FMI	NMI	PSNR	Q _{NRCTE}	TE	AG	EI	Q _{A/B/F}	Q _P	SD	SF	Q _C	Q _{IV}	Q _X	SSIM	Q _{CB}	Q _{CV}	VIF
BMPF (0.1,2)	0.047329	7.18048	0.897034	1.110096	63.33240	0.843143	317.58010	7.69027	74.92080	0.743772	0.788129	56.23580	23.30390	0.816095	0.906927	0.949038	1.663249	0.787603	118.5790	0.867904
BGSC (1.0,1)	0.037523	7.173506	0.884560	1.087714	63.90560	0.841565	220.51320	6.68554	64.93970	0.589086	0.508881	54.88060	21.03670	0.773571	0.646010	0.835154	1.622742	0.684642	21.44930	0.826569
DSFT (0.0,0)	0.042452	7.183238	0.896655	1.09095	63.29100	0.842911	207.33100	7.10156	75.83980	0.747565	0.784749	56.32360	23.64420	0.814340	0.917656	0.943182	1.658877	0.788830	78.21640	0.872679
FM (1.0,0)	0.053092	7.185199	0.895682	1.084893	63.27060	0.841046	88.24450	7.67120	75.42660	0.741902	0.778086	56.29970	23.58400	0.814678	0.912465	0.942821	1.661107	0.790410	81.06980	0.870643
OB (4.0,1)	0.045462	7.179638	0.896867	1.117892	63.28490	0.843777	286.881300	7.712189	75.78760	0.748466	0.788975	56.30070	23.67700	0.817610	0.918305	0.950064	1.660263	0.789434	113.2420	0.872385
TF (0.0,1)	0.044351	7.180714	0.897006	1.100021	63.31900	0.842044	238.296300	7.656885	75.287980	0.747829	0.791138	56.30830	23.57160	0.816977	0.921313	0.944620	1.665278	0.786408	71.29170	0.875204
ASR (1.1,0)	0.051878	7.195839	0.896024	0.941034	63.647040	0.837789	825.225200	7.495725	73.49560	0.727783	0.764038	55.71750	23.14710	0.818392	0.917409	0.921470	1.663469	0.724397	74.19540	0.848620
ASR (0.0,0)	0.063374	7.212798	0.895318	0.926963	63.34480	0.831827	324.229000	7.481720	73.57560	0.719437	0.763487	56.13900	23.00090							

the results on the Lytro dataset are presented.

1) *Qualitative performance comparison:* Figure 3 illustrates the fused images of all integrated algorithms in MFIFB on the *Lytro19* image pair. As can be seen, most algorithms can produce a clear image in this case while the BGSC and MSVD give blurring ones. To further investigate the focused/defocused boundary in the fused images, two magnified plots are given in Fig. 3 for each image. As can be seen, many algorithms cannot well handle the boundary area contained in the red box, including ASR, BGSC, CBF, DWTDE, GD, GFF, IFCNN, IFM, MFM, MGFF, MSVD, NSCT_SR, RP_SR, SFMD. Besides, some algorithms cannot fuse the boundary area contained in the green box well, including BFMF, BGSC, CBF, DCT_Corr, DCT_EOL, DWTDE, GD, IFCNN, IFM, MSVD, SFMD, SVDDCT. To sum up, the remaining methods, namely CNN, CSR, DPRL, DSIFT, ECNN, GFDF, MSR_SR, MWGF, PCANet, QB, SESF, and TF, have similar visual performances on the *Lytro19* image pair. Among these methods, five are deep learning-based methods, QB and TF are spatial domain-based methods while the rest are transform domain-based ones.

2) *Quantitative performance comparison:* Table IV lists the average value of 20 evaluation metrics for all methods on the Lytro dataset. As can be seen, the top three methods are SFMD, ECNN and GD, respectively. Specifically, GD and SFMD are transform domain-based methods while ECNN is a deep learning-based approach. This means that the transform domain-based methods achieve the best results on the Lytro dataset, and deep learning-based methods also obtain competitive results. Note that although these three methods all have the best value in three evaluation metrics, they show different characteristics. To be more specific, SFMD only performs well in image feature-based metrics, while ECNN and GD exhibit good performances in both information theory-based and human perception inspired metrics.

Actually, from the table one can find more about the performance of each kind of methods. First, the spatial domain-based approaches do not show competitive performances except TF. In transform domain-based methods, SR-based ones perform poorly in most metrics. Multi-scale-based approaches have better performance in information theory-based methods while edge-preserving-based algorithms generally perform better in image feature-based metrics. Similar to SR-based ones, the hybrid methods which combines multi-scale and SR approaches do not show good performance in most metrics. Regarding deep learning-based methods, although ECNN ranks the second among all 30 algorithms, other deep learning-based methods do not perform well. This is supervising because deep learning can provide good features and can learn fusion rules automatically. This may be because that most deep learning-based algorithms were trained using simulated multi-focus images, which are different from real-world multi-focus images, thus the generalization abilities of these algorithms are not good.

The results on Lytro dataset indicate that various MFIF algorithms may have very different performances on different evaluation metrics, therefore it is necessary to use different kinds of metrics when evaluating MFIF approaches. Besides,

although the qualitative performances are not very consistent with the overall quantitative performances, they are consistent with the human perception inspired metrics to some extent, especially Q_{CB} and Q_{CV} .

Xu et al. [36] pointed out that the defocus spread effect (DSE) is not obvious on the images of the Lytro dataset, thus the fused images produced by many algorithms have no significant visual differences. To further compare MFIF algorithms, the comparison of fusion results on the whole MFIFB dataset will be presented in the following Section.

B. Results on the whole MFIFB dataset

1) *Qualitative performance comparison:* Figure 4 presents the qualitative (visual) performance comparison of 30 fusion methods on the *MMFW12* image pair. One can see that this case is more difficult than the *Lytro19* case, since many algorithms do not produced satisfactory fused image on this image pair. To be more specific, some methods, including BGSC, CBF, CSR, DCT_Corr, DCT_EOL, DPRL, DSIFT, DWTDE, ECNN, NSCT_SR, QB, SESF, SVDDCT, and TF, have obvious visual artifacts. Besides, some algorithms show obvious color distortion, namely MGFF, MST_SR, PR_SR. Because the rest of algorithms do not show obvious visual artifacts and color distortion, thus two focused/defocused boundary areas are illustrated in the magnified plots to see more details. As can be seen, BFMF, GFDF, IFM, MFM, PCANet do not handle the boundary area contained in the red box well. Besides, BFMF, CNN, GD, GFDF, IFCNN, IFM, MFM, MSVD, PCANet and QB cannot deal with the DSE in the boundary area contained in the green box as can be seen from the magnified plots. Overall, ASR, GFF and MWGF show good performance on the *MMFW12* image pair.

2) *Quantitative performance comparison:* Table V presents the average value of 20 evaluation metrics for all methods on the whole MFIFB dataset. From the table one can see that the top three methods on the whole MFIFB dataset are QB, SFMD and GFDF, respectively. Although SFMD and QB have the same number of top three metric values, QB is ranked the first while SFMD the second. This is because that QB performs well in information theory-based, image structural similarity-based and human perception inspired metrics. In contrast, SFMD only shows good performances in image feature-based metrics but performs poorly in other kinds of metrics.

The performances of MFIF algorithms on the whole MFIF dataset are very different from that on the Lytro subset. First, the spatial domain-based approaches perform better than the transform domain-based ones. Second, deep learning-based methods have worse performances on the whole MFIFB dataset than on the Lytro dataset. Specifically, the best deep learning-based methods, namely DPRL, only ranks the fifth on the whole dataset. Apart from Lytro, the MFIFB dataset also contains other subsets such as MFFW and those proposed by Savic et al. [49] and Aymaz et al. [50]. In other words, the whole MFIFB dataset is more challenging than the Lytro dataset. The reason why the performances of deep learning-based approaches degrade is that they do not perform well on the remaining subsets in MFIFB except Lytro. For instance,

TABLE VI
 RUNNING TIME OF ALGORITHMS IN MFIFB (SECONDS PER IMAGE PAIR)

Method	Average running time	Category	Method	Average running time	Category
ASR [40]	549.95	SR-based	CBF [8]	21.11	Multi-scale-based
CSR [52]	466.27	SR-based	DCT_Corr [6]	0.34	Multi-scale-based
CNN [25]	184.78	DL-based	DCT_EOL [6]	0.24	Multi-scale-based
DRPL [30]	0.17	DL-based	DWTDE [53]	7.84	Multi-scale-based
ECNN [20]	62.92	DL-based	GD [54]	0.55	Multi-scale-based
IFCNN [10]	0.03	DL-based	MSVD [59]	0.92	Multi-scale-based
PCANet [61]	20.77	DL-based	MWGF [60]	2.76	Multi-scale-based
SESF [14]	0.16	DL-based	SVDDCT [63]	1.09	Multi-scale-based
BGSC [51]	6.52	Spatial domain-based	GFDF [55]	0.23	Edge-preserving-based
BFMF [26]	1.36	Spatial domain-based	GFF [21]	0.42	Edge-preserving-based
DSIFT [1]	7.53	Spatial domain-based	MFM [57]	1.45	Edge-preserving-based
IFM [56]	2.18	Spatial domain-based	MGFF [58]	1.17	Edge-preserving-based
QB [23]	1.07	Spatial domain-based	MST_SR [22]	0.75	Hybrid
TF [64]	0.48	Spatial domain-based	NSCT_SR [22]	91.95	Hybrid
SFMD [62]	0.81	Subspace-based	RP_SR [22]	0.81	Hybrid

the MFFW dataset has strong defocus spread effect but the simulated training data of deep learning-based methods do not have, so they cannot learn how to handle defocus spread effect.

C. Running time comparison

Table VI lists the average running time of all algorithms integrated in MFIFB. As can be seen, the running time of image fusion methods varies significantly from one to another. Generally speaking, SR-based methods are most computational expensive, which take more than 7 minutes to fuse an image pair. Besides, transform domain-based methods are generally faster than their spatial domain-based counterparts except some cases like CBF. Regarding the deep learning-based algorithms, the computational efficiency also varies greatly. For example, the running time of CNN is more than 6000 times that of IFCNN. Note that all deep learning-based algorithms in MFIFB do not update the model online.

V. CONCLUDING REMARKS

In this paper, a multi-focus image fusion benchmark (MFIFB), which includes a dataset of 105 image pairs, a code library of 30 algorithms, 20 evaluation metrics and all results is proposed. To the best of our knowledge, this is the first multi-focus image fusion benchmark to date. This benchmark facilitates better understanding of the state-of-the-art MFIF approaches and provides a platform for comparing performance among algorithms fairly and comprehensively. It should be noted that, the proposed MFIFB can be easily extended to contain more images, fusion algorithms and more evaluation metrics.

In the literature, MFIF algorithms are usually tested on a small number of images and compared with a very limited number of algorithms using just several evaluation metrics, therefore the performance comparison may not be fair and comprehensive. This makes it difficult to understand the state-of-the-art of the MFIF field and hinders the future development of new algorithms. To solve this issue, in this study extensive experiments have been carried out based on MFIFB to evaluate the performance of all integrated fusion algorithms.

We have several observations on the status of MFIF based on the experimental results. First, unlike other fields in computer vision where deep learning is almost the dominant method, deep learning methods do not provide very competitive performances on challenging MFIF datasets at the moment. Conventional methods, namely spatial domain-based and transform domain-based ones, still have good performances. This is very supervising because many deep learning-based MFIF methods were claimed to have the state-of-the-art performances. However, this is not really true on challenging MFIF dataset according to our experiments using the proposed MFIFB. The possible reason is that most deep learning-based MFIF algorithms were trained on simulated MFIF data which do not show much defocus spread effect, thus these algorithms cannot generalize well to other real-world MFIF dataset. Besides, those methods were only compared with a small number of methods using several evaluation metrics on a small dataset which does not have much defocus spread effect, thus the performances were not fully evaluated. However, due to the strong representation ability and end-to-end property of deep learning, we believe that the deep learning-based approach will be an important research direction in future. Second, a MFIF algorithm usually cannot have good performances in all aspects in terms of evaluation metrics. Some algorithms may achieve good values in information theory-based metrics while others may perform well in other kinds of metrics. Therefore, it is very important to use several kinds of evaluation metrics when conducting quantitative performance comparison for MFIF algorithms. Finally, the results of qualitative and quantitative comparisons may not be consistent for a MFIF algorithm, therefore they are both crucial when evaluating a MFIF method.

We will continue extending MFIFB by including more image pairs, algorithms and metrics. We hope that MFIFB can serve as a good starting point for researchers who are interested in multi-focus image fusion.

ACKNOWLEDGMENT

The author would like to thank Mr Shuang Xu from Xi'an Jiao Tong University for providing the MFFW dataset.

REFERENCES

- [1] Y. Liu, S. Liu, and Z. Wang, "Multi-focus image fusion with dense sift," *Information Fusion*, vol. 23, pp. 139–155, 2015.
- [2] I. De and B. Chanda, "Multi-focus image fusion using a morphology-based focus measure in a quad-tree structure," *Information Fusion*, vol. 14, no. 2, pp. 136–146, 2013.
- [3] M. Li, W. Cai, and Z. Tan, "A region-based multi-sensor image fusion scheme using pulse-coupled neural network," *Pattern Recognition Letters*, vol. 27, no. 16, pp. 1948–1956, 2006.
- [4] Q. Zhang, T. Shi, F. Wang, R. S. Blum, and J. Han, "Robust sparse representation based multi-focus image fusion with dictionary construction and local spatial consistency," *Pattern Recognition*, vol. 83, pp. 299–313, 2018.
- [5] Q. Zhang, Y. Liu, R. S. Blum, J. Han, and D. Tao, "Sparse representation based multi-sensor image fusion for multi-focus and multi-modality images: A review," *Information Fusion*, vol. 40, pp. 57–75, 2018.
- [6] M. Amin-Naji and A. Aghagolzadeh, "Multi-focus image fusion in dct domain using variance and energy of laplacian and correlation coefficient for visual sensor networks," *Journal of AI and Data Mining*, vol. 6, no. 2, pp. 233–250, 2018.
- [7] L. Kou, L. Zhang, K. Zhang, J. Sun, Q. Han, and Z. Jin, "A multi-focus image fusion method via region mosaicking on laplacian pyramids," *PloS one*, vol. 13, no. 5, 2018.
- [8] B. K. Shreyamsha Kumar, "Image fusion based on pixel significance using cross bilateral filter," *Signal, Image and Video Processing*, vol. 9, no. 5, pp. 1193–1204, Jul 2015.
- [9] H. Zhai and Y. Zhuang, "Multi-focus image fusion method using energy of laplacian and a deep neural network," *Applied Optics*, vol. 59, no. 6, pp. 1684–1694, 2020.
- [10] Y. Zhang, Y. Liu, P. Sun, H. Yan, X. Zhao, and L. Zhang, "IFCNN: A general image fusion framework based on convolutional neural network," *Information Fusion*, vol. 54, no. August 2018, pp. 99–118, 2020.
- [11] C. Wang, Z. Zhao, Q. Ren, Y. Xu, and Y. Yu, "A novel multi-focus image fusion by combining simplified very deep convolutional networks and patch-based sequential reconstruction strategy," *Applied Soft Computing*, p. 106253, 2020.
- [12] H. Xu, F. Fan, H. Zhang, Z. Le, and J. Huang, "A deep model for multi-focus image fusion based on gradients and connected regions," *IEEE Access*, vol. 8, pp. 26 316–26 327, 2020.
- [13] X. Yan, S. Z. Gilani, H. Qin, and A. Mian, "Unsupervised deep multi-focus image fusion," *arXiv preprint arXiv:1806.07272*, 2018.
- [14] B. Ma, X. Ban, H. Huang, and Y. Zhu, "Sesf-fuse: An unsupervised deep model for multi-focus image fusion," *arXiv preprint arXiv:1908.01703*, 2019.
- [15] H. T. Mustafa, F. Liu, J. Yang, Z. Khan, and Q. Huang, "Dense multi-focus fusion net: A deep unsupervised convolutional network for multi-focus image fusion," in *International Conference on Artificial Intelligence and Soft Computing*. Springer, 2019, pp. 153–163.
- [16] H. Jung, Y. Kim, H. Jang, N. Ha, and K. Sohn, "Unsupervised Deep Image Fusion with Structure Tensor Representations," *IEEE Transactions on Image Processing*, vol. 29, pp. 3845–3858, 2020.
- [17] H. Li, R. Nie, D. Zhou, and X. Gou, "Convolutional neural network based multi-focus image fusion," in *Proceedings of the 2018 2nd International Conference on Algorithms, Computing and Systems*, 2018, pp. 148–154.
- [18] C. Du and S. Gao, "Image segmentation-based multi-focus image fusion through multi-scale convolutional neural network," *IEEE access*, vol. 5, pp. 15 750–15 761, 2017.
- [19] X. Guo, R. Nie, J. Cao, D. Zhou, L. Mei, K. He, S. Member, R. Nie, J. Cao, and D. Zhou, "FuseGAN: Learning to fuse Multi-focus Image via Conditional Generative Adversarial Network," *IEEE Transactions on Multimedia*, vol. 21, no. 8, pp. 1–1, 2019.
- [20] M. Amin-Naji, A. Aghagolzadeh, and M. Ezoji, "Ensemble of CNN for Multi-Focus Image Fusion," *Information Fusion*, vol. 51, no. February, pp. 201–214, 2019.
- [21] S. Li, X. Kang, and J. Hu, "Image fusion with guided filtering," *IEEE Transactions on Image processing*, vol. 22, no. 7, pp. 2864–2875, 2013.
- [22] Y. Liu, S. Liu, and Z. Wang, "A general framework for image fusion based on multi-scale transform and sparse representation," *Information Fusion*, vol. 24, pp. 147–164, 2015.
- [23] X. Bai, Y. Zhang, F. Zhou, and B. Xue, "Quadtree-based multi-focus image fusion using a weighted focus-measure," *Information Fusion*, vol. 22, pp. 105–118, 2015.
- [24] Q. Zhang and M. D. Levine, "Robust multi-focus image fusion using multi-task sparse representation and spatial context," *IEEE Transactions on Image Processing*, vol. 25, no. 5, pp. 2045–2058, 2016.
- [25] Y. Liu, X. Chen, H. Peng, and Z. Wang, "Multi-focus image fusion with a deep convolutional neural network," *Information Fusion*, vol. 36, pp. 191–207, 2017.
- [26] Y. Zhang, X. Bai, and T. Wang, "Boundary finding based multi-focus image fusion through multi-scale morphological focus-measure," *Information fusion*, vol. 35, pp. 81–101, 2017.
- [27] H. Tang, B. Xiao, W. Li, and G. Wang, "Pixel convolutional neural network for multi-focus image fusion," *Information Sciences*, vol. 433, pp. 125–141, 2018.
- [28] M. S. Farid, A. Mahmood, and S. A. Al-Maadeed, "Multi-focus image fusion using content adaptive blurring," *Information fusion*, vol. 45, pp. 96–112, 2019.
- [29] O. Bouzos, I. Andreadis, and N. Mitianoudis, "Conditional random field model for robust multi-focus image fusion," *IEEE Transactions on Image Processing*, vol. 28, no. 11, pp. 5636–5648, 2019.
- [30] J. Li, X. Guo, G. Lu, B. Zhang, Y. Xu, F. Wu, and

- D. Zhang, “Drpl: Deep regression pair learning for multi-focus image fusion,” *IEEE Transactions on Image Processing*, vol. 29, pp. 4816–4831, 2020.
- [31] H. Xu, J. Ma, Z. Le, J. Jiang, and X. Guo, “Fusiondn: A unified densely connected network for image fusion,” in *Thirty-Fourth AAAI Conference on Artificial Intelligence*, 2020.
- [32] H. Zhang, H. Xu, Y. Xiao, X. Guo, and J. Ma, “Re-thinking the image fusion: A fast unified image fusion network based on proportional maintenance of gradient and intensity,” in *Proceedings of the AAAI Conference on Artificial Intelligence*, 2020.
- [33] M. Nejati, S. Samavi, and S. Shirani, “Multi-focus image fusion using dictionary-based sparse representation,” *Information Fusion*, vol. 25, pp. 72–84, 2015.
- [34] Y. Wu, J. Lim, and M.-H. Yang, “Object tracking benchmark,” *IEEE Transactions on Pattern Analysis and Machine Intelligence*, vol. 37, no. 9, pp. 1834–1848, 2015.
- [35] M. Kristan, J. Matas, A. Leonardis, T. Vojir, R. Pflugfelder, G. Fernandez, G. Nebehay, F. Porikli, and L. Čehovin, “A novel performance evaluation methodology for single-target trackers,” *IEEE Transactions on Pattern Analysis and Machine Intelligence*, vol. 38, no. 11, pp. 2137–2155, Nov 2016.
- [36] S. Xu, X. Wei, C. Zhang, J. Liu, and J. Zhang, “Mffw: A new dataset for multi-focus image fusion,” *arXiv preprint arXiv:2002.04780*, 2020.
- [37] X. Deng and P. L. Dragotti, “Deep Convolutional Neural Network for Multi-modal Image Restoration and Fusion,” pp. 1–15, 2019.
- [38] G.-P. Fu, S.-H. Hong, F.-L. Li, and L. Wang, “A novel multi-focus image fusion method based on distributed compressed sensing,” *Journal of Visual Communication and Image Representation*, vol. 67, p. 102760, 2020.
- [39] B. Yang and S. Li, “Multifocus image fusion and restoration with sparse representation,” *IEEE Transactions on Instrumentation and Measurement*, vol. 59, no. 4, pp. 884–892, 2010.
- [40] Y. Liu and Z. Wang, “Simultaneous image fusion and denoising with adaptive sparse representation,” *IET Image Processing*, vol. 9, no. 5, pp. 347–357, 2014.
- [41] W.-W. Wang, P.-L. Shui, and G.-X. Song, “Multifocus image fusion in wavelet domain,” in *Proceedings of the 2003 International Conference on Machine Learning and Cybernetics (IEEE Cat. No. 03EX693)*, vol. 5. IEEE, 2003, pp. 2887–2890.
- [42] J. Zhi-guo, H. Dong-bing, C. Jin, and Z. Xiao-kuan, “A wavelet based algorithm for multi-focus micro-image fusion,” in *Third International Conference on Image and Graphics (ICIG’04)*. IEEE, 2004, pp. 176–179.
- [43] D. P. Bavisetti, G. Xiao, and G. Liu, “Multi-sensor image fusion based on fourth order partial differential equations,” in *2017 20th International Conference on Information Fusion (Fusion)*. IEEE, 2017, pp. 1–9.
- [44] Y. Chen, J. Guan, and W.-K. Cham, “Robust multi-focus image fusion using edge model and multi-matting,” *IEEE Transactions on Image Processing*, vol. 27, no. 3, pp. 1526–1541, 2017.
- [45] W. Zhao, H. Lu, and D. Wang, “Multisensor image fusion and enhancement in spectral total variation domain,” *IEEE Transactions on Multimedia*, vol. 20, no. 4, pp. 866–879, 2017.
- [46] W. Zhao, D. Wang, and H. Lu, “Multi-focus image fusion with a natural enhancement via a joint multi-level deeply supervised convolutional neural network,” *IEEE Transactions on Circuits and Systems for Video Technology*, vol. 29, no. 4, pp. 1102–1115, 2018.
- [47] Y. Yang, Z. Nie, S. Huang, P. Lin, and J. Wu, “Multilevel features convolutional neural network for multifocus image fusion,” *IEEE Transactions on Computational Imaging*, vol. 5, no. 2, pp. 262–273, 2019.
- [48] V. Deshmukh, A. Khaparde, and S. Shaikh, “Multi-focus image fusion using deep belief network,” in *International Conference on Information and Communication Technology for Intelligent Systems*. Springer, 2017, pp. 233–241.
- [49] S. Savić and Z. Babić, “Multifocus image fusion based on empirical mode decomposition,” in *19th IEEE International Conference on Systems, Signals and Image Processing (IWSSIP)*, 2012.
- [50] S. Aymaz, C. Köse, and Ş. Aymaz, “Multi-focus image fusion for different datasets with super-resolution using gradient-based new fusion rule,” *Multimedia Tools and Applications*, pp. 1–40, 2020.
- [51] J. Tian, L. Chen, L. Ma, and W. Yu, “Multi-focus image fusion using a bilateral gradient-based sharpness criterion,” *Optics communications*, vol. 284, no. 1, pp. 80–87, 2011.
- [52] Y. Liu, X. Chen, R. K. Ward, and Z. J. Wang, “Image fusion with convolutional sparse representation,” *IEEE signal processing letters*, vol. 23, no. 12, pp. 1882–1886, 2016.
- [53] Y. Liu and Z. Wang, “Multi-focus image fusion based on wavelet transform and adaptive block,” *Journal of image and graphics*, vol. 18, no. 11, pp. 1435–1444, 2013.
- [54] S. Paul, I. S. Sevcenco, and P. Agathoklis, “Multi-exposure and multi-focus image fusion in gradient domain,” *Journal of Circuits, Systems and Computers*, vol. 25, no. 10, p. 1650123, 2016.
- [55] X. Qiu, M. Li, L. Zhang, and X. Yuan, “Guided filter-based multi-focus image fusion through focus region detection,” *Signal Processing: Image Communication*, vol. 72, pp. 35–46, 2019.
- [56] S. Li, X. Kang, J. Hu, and B. Yang, “Image matting for fusion of multi-focus images in dynamic scenes,” *Information Fusion*, vol. 14, no. 2, pp. 147–162, 2013.
- [57] J. Ma, Z. Zhou, B. Wang, and M. Dong, “Multi-focus image fusion based on multi-scale focus measures and generalized random walk,” in *2017 36th Chinese Control Conference (CCC)*. IEEE, 2017, pp. 5464–5468.
- [58] D. P. Bavisetti, G. Xiao, J. Zhao, R. Dhuli, and G. Liu, “Multi-scale guided image and video fusion: A fast and efficient approach,” *Circuits, Systems, and Signal Processing*, vol. 38, no. 12, pp. 5576–5605, Dec 2019.
- [59] V. Naidu, “Image fusion technique using multi-resolution singular value decomposition,” *Defence Science Journal*,

- vol. 61, no. 5, pp. 479–484, 2011.
- [60] Z. Zhou, S. Li, and B. Wang, “Multi-scale weighted gradient-based fusion for multi-focus images,” *Information Fusion*, vol. 20, pp. 60–72, 2014.
- [61] X. Song and X.-J. Wu, “Multi-focus Image Fusion with PCA Filters of PCANet,” in *IAPR Workshop on Multimodal Pattern Recognition of Social Signals in Human-Computer Interaction*. Springer, 2018, pp. 1–17.
- [62] H. Li, L. Li, and J. Zhang, “Multi-focus image fusion based on sparse feature matrix decomposition and morphological filtering,” *Optics Communications*, vol. 342, pp. 1–11, 2015.
- [63] M. Amin-Naji, P. Ranjbar-Noiey, and A. Aghagolzadeh, “Multi-focus image fusion using singular value decomposition in dct domain,” in *2017 10th Iranian Conference on Machine Vision and Image Processing (MVIP)*. IEEE, 2017, pp. 45–51.
- [64] J. Ma, Z. Zhou, B. Wang, L. Miao, and H. Zong, “Multi-focus image fusion using boosted random walks-based algorithm with two-scale focus maps,” *Neurocomputing*, vol. 335, pp. 9–20, 2019.
- [65] Z. Liu, E. Blasch, Z. Xue, J. Zhao, R. Laganier, and W. Wu, “Objective assessment of multiresolution image fusion algorithms for context enhancement in night vision: A comparative study,” *IEEE Transactions on Pattern Analysis and Machine Intelligence*, vol. 34, pp. 94–109, 2012.
- [66] D. M. Bulanon, T. Burks, and V. Alchanatis, “Image fusion of visible and thermal images for fruit detection,” *Biosystems Engineering*, vol. 103, no. 1, pp. 12–22, 2009.
- [67] V. Aardt and Jan, “Assessment of image fusion procedures using entropy, image quality, and multispectral classification,” *Journal of Applied Remote Sensing*, vol. 2, no. 1, p. 023522, 2008.
- [68] M. Hossny, S. Nahavandi, and D. Creighton, “Comments on ‘information measure for performance of image fusion’,” *Electronics letters*, vol. 44, no. 18, pp. 1066–1067, 2008.
- [69] P. Jagalingam and A. V. Hegde, “A review of quality metrics for fused image,” *Aquatic Procedia*, vol. 4, no. 1cwrcoe, pp. 133–142, 2015.
- [70] Q. Wang, Y. Shen, and J. Q. Zhang, “A nonlinear correlation measure for multivariable data set,” *Physica D: Nonlinear Phenomena*, vol. 200, no. 3-4, pp. 287–295, 2005.
- [71] Q. Wang, Y. Shen, and J. Jin, “Performance evaluation of image fusion techniques,” *Image fusion: algorithms and applications*, vol. 19, pp. 469–492, 2008.
- [72] N. Cvejic, C. Canagarajah, and D. Bull, “Image fusion metric based on mutual information and tsallis entropy,” *Electronics letters*, vol. 42, no. 11, pp. 626–627, 2006.
- [73] G. Cui, H. Feng, Z. Xu, Q. Li, and Y. Chen, “Detail preserved fusion of visible and infrared images using regional saliency extraction and multi-scale image decomposition,” *Optics Communications*, vol. 341, pp. 199–209, 2015.
- [74] B. Rajalingam and R. Priya, “Hybrid multimodality medical image fusion technique for feature enhancement in medical diagnosis,” *International Journal of Engineering Science Invention*, 2018.
- [75] C. S. Xydeas and P. V. V., “Objective image fusion performance measure,” *Military Technical Courier*, vol. 36, no. 4, pp. 308–309, 2000.
- [76] J. Zhao, R. Laganier, and Z. Liu, “Performance assessment of combinative pixel-level image fusion based on an absolute feature measurement,” *International Journal of Innovative Computing, Information and Control*, vol. 3, no. 6, pp. 1433–1447, 2007.
- [77] Y.-J. Rao, “In-fibre bragg grating sensors,” *Measurement science and technology*, vol. 8, no. 4, p. 355, 1997.
- [78] A. M. Eskicioglu and P. S. Fisher, “Image quality measures and their performance,” *IEEE Transactions on communications*, vol. 43, no. 12, pp. 2959–2965, 1995.
- [79] N. Cvejic, A. Loza, D. Bull, and N. Canagarajah, “A similarity metric for assessment of image fusion algorithms,” *International journal of signal processing*, vol. 2, no. 3, pp. 178–182, 2005.
- [80] G. Piella and H. Heijmans, “A new quality metric for image fusion,” in *Proceedings 2003 International Conference on Image Processing (Cat. No. 03CH37429)*, vol. 3. IEEE, 2003, pp. III–173.
- [81] C. Yang, J.-Q. Zhang, X.-R. Wang, and X. Liu, “A novel similarity based quality metric for image fusion,” *Information Fusion*, vol. 9, no. 2, pp. 156–160, 2008.
- [82] Z. Wang, A. C. Bovik, H. R. Sheikh, E. P. Simoncelli *et al.*, “Image quality assessment: from error visibility to structural similarity,” *IEEE transactions on image processing*, vol. 13, no. 4, pp. 600–612, 2004.
- [83] Y. Chen and R. S. Blum, “A new automated quality assessment algorithm for image fusion,” *Image and vision computing*, vol. 27, no. 10, pp. 1421–1432, 2009.
- [84] H. Chen and P. K. Varshney, “A human perception inspired quality metric for image fusion based on regional information,” *Information fusion*, vol. 8, no. 2, pp. 193–207, 2007.
- [85] Y. Han, Y. Cai, Y. Cao, and X. Xu, “A new image fusion performance metric based on visual information fidelity,” *Information Fusion*, vol. 14, no. 2, pp. 127–135, 2013.
- [86] J. Ma, Y. Ma, and C. Li, “Infrared and visible image fusion methods and applications: A survey,” *Information Fusion*, vol. 45, pp. 153–178, 2019.